Dear Prof. Richard Perham,

I am submitting a manuscript entitled to "**Engineered dimer interface mutants of Triosephosphate isomerase: The role of inter subunit interactions in enzyme function and stability",** to be considered for publication in the FEBS journal.

Sincerely,
Prof. P. Balaram.

Engineered dimer interface mutants of Triosephosphate isomerase: The role of inter subunit interactions in enzyme function and stability

Mousumi Banerjee.[‡], Hemalatha Balaram.[§], N. V Joshi [†], P. Balaram, [‡*],

[‡]Molecular Biophysics Unit, Indian Institute of Science, Bangalore – 560012, India.

[§]Molecular Biology and Genetics Unit, Jawaharlal Nehru Centre for Advanced Scientific Research, Jakkur, Bangalore – 560064, India.

[†] Centre for Ecological Sciences. Indian Institute of Science, Bangalore – 560012, India

[*] Address for correspondence:

Prof. P. Balaram

Molecular Biophysics Unit, Indian Institute of Science

Bangalore – 560 012, India.

Ph: +91-80-22932337, Fax: +91-80-23600535

Email: pb@mbu.iisc.ernet.in

Running title :

Abbreviations

PfTIM- *Plasmodium falciparum* triosephosphate isomerase

TbTIM- *Trypanosoma brucei* triosephosphate isomerase

TcTIM- *Trypanosoma cruzi* triosephosphate isomerase

C13D- PfTIM Cys 13 to Asp mutant

C13E- PfTIM Cys 13 to Glu mutant

EC number for triosephosphate isomerase: 5.3.1.1

Keywords

Dimer stability, Subunit interface, *Plasmodium falciparum*, Triosephosphate isomerase, Inter subunit interactions.

Subdivision: Enzyme and catalysis

Abstract:

The role of inter subunit interactions in maintaining optimal catalytic activity in triosephosphate isomerase has been probed, using the *Plasmodium falciparum* enzyme as a model. Examination of subunit interface contacts in the crystal structures suggest that, residue 75 (Thr, conserved) and residue 13 (Cys, variable) make the largest number of inter subunit contacts. The mutants C13D and C13E have been constructed and display significant reduction in catalytic activity as compared to wild type enzyme (a ~7.4 fold decrease in k_{cat} for the C13D and ~3.3 fold for the C13E mutants). Analytical gel filtration demonstrate that the C13D dissociates at the concentration <1.25 μM whereas TWT and C13E retains the dimeric structure. The order of stability to chemical denaturants, urea and guanidium chloride, an irreversible thermal denaturation follows the order TWT>C13E>C13D. Modeling studies establish that the C13D mutation is likely to cause a significant greater structural perturbation than C13E. Analysis of sequence and structural data for TIMs from diverse sources suggests that residues 13 and 82 from a pair of proximal sites, in which a limited number of residue pairs may be accommodated.

Introduction

Triosephosphate isomerase (TIM) catalyses the reversible isomerisation of dihydroxyacetone phosphate (DHAP) and glyceraldehyde 3-phosphate (GAP) a central step in the glycolytic pathway [1]. This deceptively simple chemical reaction requires the stereospecific abstraction of a proton bonded to a carbon atom followed by re-protonation at the adjacent carbon atom [2-5]. Extensive structural, kinetic and mutagenesis studies have provided a detailed picture of the mechanism leading Jeremy Knowles to call TIM "an evolutionary perfect enzyme" [6, 7]. Despite the extensive dissection of the TIM mechanism [8,9], protein design experiments to engineer TIM active sites on to other protein scaffolds have proved unsuccessful [10,11]. TIM functions as a dimeric enzyme in bacteria and eukaryotes, while the archaeal enzyme is a tetramer, as demonstrated by studies on the proteins from *Pyrococcus woesei* and *Methanocaldococcus jannaschii* [12-16]. Several studies have attempted to address the question of whether TIM is an obligate dimer. Attempts to engineer monomeric TIMs have resulted in well folded (α_8/β_8) barrel structures, whose catalytic activity is reduced by over 1000 fold [16, 17]. The critical residues at the TIM active site, Lys12, His95 and Glu165, which surround the substrate, are all located on one subunit. The availability of a high resolution crystal structure of the yeast TIM-DHAP complex (PDB ID 1NEY) [18] provides many insights into the positioning of the substrate with respect to key catalytic residues involved in the proton transfer reaction. The sharp fall in interactions in engineered monomers suggests that functional active site construction must involve critical interactions at the subunit interface. Figure 1 schematically summarizes the peptide segments which provide a maximum number of inter-subunit contacts (≤ 4Å) in the enzyme from *Plasmodium*

falciparum TIM (PfTIM) [19, 20]. Bacterial and eukaryotic TIMs have a polypeptide chain length of 240-270 residues, with PfTIM having a length of 248 residues. The segments comprising the dimer interface lie within the first 100 residues. Four distinct segments may be identified which comprise the interacting surface.

A feature of the malarial parasite enzyme, also present in the enzymes from trypanosomal and leishmania, is the occurrence of a Cys residue at position 13 adjacent to the active site Lys12 residue [21, 22] (We use here the residue numbering scheme for the *Plasmodium falciparum* enzyme. Numbering scheme for PfTIM and yeast TIM are identical for the fragments 1-32 and 58-248. Residue 34-57 of PfTIM corresponds to residue 33-56 of Yeast TIM).). In the human enzyme Met occurs at this position leading to attempts to develop sulfydryl modifiers as site directed inhibitors [23-26]. Inspection of Figure 1 reveals that the largest number of interface contacts is made by the fully conserved Thr75 residue, which is important in maintaining active site architecture and Cys13, which is a variable residue in sequences from other organisms. A double mutant, constructed by Wierenga and coworkers, derived by replacement of T75 and G76 by R75 and E76 resulted in a monomeric protein in solution (known as RE mutant), with reduced catalytic activity compared to the wild type (k_{cat} for WT =3.7X 10^5 min^{-1} and k_{cat} for RE mutant = 1.3 X 10^2 min^{-1}) [12]. Figure 2 shows a view of the inter subunit interaction involving the Cys13 residue and the loop 3 segment (residues 71-79) in PfTIM. It is evident that multiple hydrogen bonding interactions involving the Cys13 backbone and the thiol S-H group may contribute to the stability of the dimer. Multiple sequence alignment of a curated dataset of 470 non-archeal TIM sequences revealed the distribution of residues at position 13, summarized in Figure 2 (inset). In the

overwhelming majority of sequences Methionine (Met) occurs at this position, while 7 other residues are also seen. The absence of charged and aromatic amino acids is striking. We therefore chose to examine the effects of introducing the negatively charged residues Asp (D) and Glu (E) in order to probe effects on dimer stability and enzymatic activity.

Results

Kinetic parameters

The steady state kinetics for wild type and residue 13 mutants of *Pf*TIM was measured by a coupled enzyme assay, using glyceraldehyde 3-phosphate (GAP) as a substrate. The k_{cat}, K_m values for the wild type enzyme, C13D and C13E mutants are listed in Table1. The enzymes from the parasites *Trypanosoma brucei and Trypanosoma cruzi* also contain a cysteine residue at the structurally equivalent position (*T. brucei* C14, *T. cruzi* C15). Earlier studies by Hernandez-Alcantara *et al*., (2002) [27] and Zomosa-Signoret *et al*., (2007) [28] have reported mutational studies at this position on the *T. brucei* (TbTIM) and heterodimers of *T.brucei-T.cruzi* subunits harboring a C15A mutation. The kinetic data reported for these mutants is also listed in Table1 for comparison. In these cases Cys was replaced by neutral polar and hydrophobic residues [29, 30]. Inspection of the data in Table1 reveals that the C13D mutant shows a ~7.4 fold loss of activity, while the drop at k_{cat} in ~3.3 fold for the C13E mutant. In both the cases there is no significant change in K_m as compared to wild type enzyme. The previously published data for the TbTIM suggests that the replacement of Cys14 with Ala, Pro, Ser, Thr and Val has little effect on enzymatic activity. In contrast the C14F mutant shows a significant reduction (~ 216 fold) in k_{cat} and a 10 fold increase in K_m [29]. These results

establish that substrate binding is not appreciably affected in the C13D and C13E mutants, while k_{cat} shows a significant reduction.

Anallytical gel filtration

Figure 3 shows the analytical gel filtration profiles for WT, C13D and C13E mutants. At a concentration of 1.25 μM the wild type enzyme has an elution volume ~13.9 ml, corresponding to a dimer. The C13E and C13D mutants also eluted at the same position at a concentration of 2.5 μM, indicating that under these condition the dimeric structure was retained. At this concentration the C13E mutant also shows a single peak with the same elution volume, suggesting that the mutation has not interfered with the dimerization. In sharp contrast, the C13D shows a single peak (13.9 ml) corresponding to the dimer at 2.5 μM, whereas the lower concentration of 1.25 μM protein elutes at 15.5 ml. This suggests that the C13D mutation appears to destabilize the dimer interface resulting in subunit dissociation. In an earlier report from this laboratory a sharp fall in measured enzymatic activity was observed in the concentration range 0.2 uM – 0.6 uM for the C13D mutant [20].

Effect of chemical denaturants

The $(\beta/\alpha)_8$ barrel structure in PfTIM retains considerable secondary and tertiary structure even in presence of 8M urea. However, the protein has been shown to unfold readily in presence of guanidium chloride (Gdmcl) solutions, at a denaturant concentration ~2.5M [31]. Unfolding may be conveniently monitored by measuring the fluorescence emission spectrum which arises from contributions due to Trp11 and

Trp168 [32]. Figure 4 (A and C) compare the change in fluorescence as a function of emission maxima (λ_{max}) for urea and guanidium concentration for TWT, C13D and C13E mutants. The emission maximum of WT and the C13D mutant is 331 nm, while the λ_{max} for the C13E mutant is 333 nm. Upon addition of urea all three proteins show a shift of the emission maxima to a longer wavelength suggested a solvent exposure of the Trp side chains. In the case of TWT this red shift of emission is observed only in urea concentration >5M. In sharp contrast, the change in fluorescence properties occurs at a significantly lower concentration (2-4M) in the case of C13D and C13E mutants. Evidently, weakening of subunit interface interactions contributes appreciably in determining the midpoint (C_m) of urea denaturation process. Interestingly, in the case of guanidium chloride (Gdmcl) the distinction between the three proteins is less dramatic although a midpoint of the unfolding transition follows the order TWT>C13E> C13D. Figure 4 (B and D) summarizes unfolding profiles obtained with the three proteins in urea and guanidium chloride solution using CD ellipticity at 222 nm (θ_{222}) as a probe. It is clearly seen that the order of stability in urea solution is TWT>C13E> C13D. The similar conclusion may be drawn from the guanidium chloride data (Figure 4D).

Thermal denaturation

PfTIM wild type undergoes irreversible thermal precipitation at ~60 °C, a process attributed to the formation of protein aggregates through unfolding intermediates [33]. This process can be conveniently monitored by observing the drop in CD ellipticity at 222nm (θ_{222}) or the increase in Rayleigh scattering upon aggregation. Figure 5 compares the changes in ellipticity for PfTIM wild type and the mutants C13D and C13E. It is

clearly evident that the mutants undergo thermal denaturation at much lower temperatures, with the C13D mutant being the most fragile. The measured melting temperature (T_m °C) are listed in Table1, which also provides comparative data obtained previously for trypanosomal TIMs. The C13D mutant is appreciably less stable than the C13E, consistent with the results obtained for chemical denaturation. Indeed, the C13D mutant has the lowest T_m value, 43.8 °C, of all the mutants listed in Table1.

Discussion:

The kinetic and spectroscopic data presented above established that the introduction of a negatively charged residue at position 13 in PfTIM results in catalytic impaired mutants, which also display a significantly lower degree of structural stability. The analytical gel filtration further suggests that the C13D mutant shows a significantly enhanced tendency to dissociate into monomers. The vast body of structural data on TIM from different sources has established that dimerization is indeed critical for maintenance of enzymatic activity. Attempts to monomerize TIM have resulted in the engineering of structurally stable mono-TIMs [16, 17] which however, have catalytic activities that are reduced by a factor of 1000 as compared to the native enzyme. Inspection of the crystal structure reveals that the completely conserved Thr75 residues makes crucial hydrogen bonding contacts with the other subunit which appears to be essential for holding the active site residues in an appropriate geometry (Figure 6) [34]. Figure 2 shows a view of residue C13 and the close contact that it makes with loop3 residues (69-79) from the neighboring subunit. The availability of a large number of TIM sequences from diverse organisms prompted us to examine the nature of residues occurring at this position and proximal

interacting sites on the proteins. Figure 2 (inset) summarizes a survey of 470 (eukaryotic and bacteria) TIM sequences which reveals that position 13 is largely occupied by apolar amino acid residues like Met and Leu, with very few examples of polar residues. Significantly, there are no reported occurrences of positively charged residues at this position. The sulfur atom of Cys13 appears to be close packed with Ser79 and Ile82 side chains as seen in Figure 7. In order to examine the steric perturbation caused by the C13D and C13E mutations we modeled the side chains at position 13 and examined contacts made for various rotameric states, chosen from a library (Figure 8). Interestingly, the carboxylate of Asp13 is positioned to make a reasonably good hydrogen bond contact with the backbone NH group of Ser79. However, short contacts are observed with the C^{δ} methyl group of Ile82. In contrast, the more extended Glu13 side chain can be accommodated at this position without this unfavorable contact. An unacceptably short hydrogen bond distance to Ser79 may be relieved by minor conformational adjustments. The modeling result suggests that the C13D mutation is anticipated to result in greater structural perturbation than the C13E mutation. This is indeed, consistent with the experimental results where a significant greater drop in k_{cat} (~7.4 fold) is observed for the C13D mutant, while the fall in activity is lower for the C13E mutant (~3.3 fold). The greater tendency of the C13D mutant to dissociate lends further support to the conclusion that introduction of smaller aspartyl side chain results in a greater perturbation than the larger glutamyl side chain at this position. Figure 8 shows a view of the conserved residues of TIM oriented about the substrate DHAP [18]. The Lys12 residue is critical for activity and is held in place by Asn10 and Gln64 both of which are almost completely conserved in all TIM sequences. Indeed in the 470

(bacterial, eukaryotic) dataset position 64 is occupied by Gln in 442 and Glu in 28 whereas residue 10 has Asn in 465 and Ser in 5 sequences. The Glu-Gln and Asn-Ser replacements will leave the hydrogen bonds to the Lys backbone unaffected. This feature appears to be critical in maintaining TIM activity, since the Lys 12 residue adopts unusual Ramachandran ϕ, ψ values ($\phi = 54.3 \pm 5.5$, $\psi = -144.1 \pm 7.0$) in all 24 crystal structures from different organisms determined thus far [34]. Residue 13, the site of mutation in the present study is adjacent in sequence to this critical residue as seen in Figure 9.

Inspection of Figure 7 suggests that the inter-residue 13(A)/82(B) interaction across the subunit interface may make an important contribution to dimer stability and enzymatic activity. Using the 470 sequence dataset we note that the following 13(A)/82(B) doublets are observed M/M 259, L/M 54, M/Q 33, N/A 33, C/M 14, M/V 13, M/F 11. These account for 374 examples of the total dataset. Both the positions do not contain a charged residue. There are 4 examples of the C/I doublet observed in the enzymes from *P. falciparum*, *T. brucei*, *T. cruzi* and *L. mexicana.* Interestingly, crystal structures are available in all the cases. In the natural sequences accommodation of a Cys residue at position 13 (22 examples) results in only Met (14), Ile (4), His (3) and Gln (1). Crystal structures are available for the C13/M82 pair (3 examples) and C13/I82 pair (4 examples). Despite the apparent diversity of residues at this position it is clear that only limited numbers of pairs are in fact compatible for the requirements of subunit assembly and enzyme activity. The three example of the doublet Q13/Q82 are of special interest since the side chain would resemble the Glu side chain introduced in the present study; at this position. In all three cases 13A/82B pairs are from three different organisms like,

Moraxella (a bacterium that infects the respiratory tract), *Psychrobacter arcticus* and *Psychrobacter cryohalolentis*. Structural analyses of these TIMs or of the engineered double mutants should provide further insights.

Despite the complete exclusion of charged amino acids at position 13 in TIM sequences the engineered C13E mutant is only about 3 fold less active than the wild type enzyme. Figure 10 provides a comparison of the k_{cat} value reported for TIMs from diverse organisms. The lowest reported value as far is for *Helicobactor pylori* which has $k_{cat} \sim 1.46 \times 10^3\ s^{-1}$ [35]. The measured activity for the C13E mutant is clearly below the threshold for all naturally occurring TIMs studied at the present time suggesting that impaired catalytic activity may be selected out if it significantly affects the flux of glycolysis in an organism. Mutational analysis guided by comparisons between the growing numbers of natural sequences may be valuable in identifying coevolving segments of proteins [36] which are important for the maintenance of structure and function.

Materials:

All media components were purchased from HiMedia Laboratories (Mumbai, India). Substrates used for enzyme assays, buffer components, protein molecular weight markers, urea and guanidine hydrochloride were purchased from Sigma Chemical Company (St. Louis, MO, USA). All reagents were of analytical grade. Akta Basic HPLC, Superdex 200 and Q-sepharose columns were from GE healthcare (India). All assays were done using Jasco-710 (Tokyo, Japan) spectrophotometer and JASCO-715 spectro-polarimeter (Tokyo, Japan) fitted with a water circulated cell holder. The

temperature was maintained using Julabo (JULABO Labortechnik GmbH, Seelbach, Germany) circulating water bath.

Site directed mutagenesis

Wild type PfTIM gene was cloned in pTrc99A vector and expressed in AA200 *E. coli* cells (TIM null mutants) [37]. The Asp (D) and Glu (E) mutants at position 13 were generated using "Megaprimer" PCR method [38]. The oligonucleotides used in this study are -

C13D: 5′CCACATGGCTAGAAAATATTTTGTCGCAGCAAACTGGAAAGAAAT GGAACT3′ and C13E: 5′CACCATGGCTAGAAAATATTTTGTCG CAGCAAA CTGGAAAGAAAATGGA-3′. Briefly, the mutants were generated using two rounds of PCR. In the 1st round the megaprimer was generated along with the mutation and in the 2nd round the full length gene was amplified using the C-terminal wild type primer of TIM gene. The PCR mix contained 200 ng of each primer, 20 ng of the template, 200 μM of each dNTP and 5 units of *Taq* DNA polymerase for a 50 μl reaction. The PCR cycle used was denaturation at 94 °C for 4 min to give a hot start, then 93 °C for 25 sec, annealing at 48 °C for 50 sec and extension at 73 °C for 35 sec. The product obtained, after 30 cycles of PCR, was purified by elution from agarose gels and used as a mega primer in a second round of PCR. The other primer S used in the PCR amplification are

TIM forward primer – 5′-CAGAATTCCATGGCTAGAAAATATTTTGTCGC-3′

TIM reverse primer - 5′-ACGGATCCTTACATAGCACTTTTTATTATATC-3′

The 2nd PCR condition was 94 °C for 4 min to give a hot start, then 93 °C for 30 sec, annealing at 52 °C for 50 sec and extension at 73 °C for 1min. After 30 cycles a final

extension of 10min at 72 °C was allowed. The full-length amplified product containing the desired mutation was purified using gene cleaning kit (QIAGEN), digested with enzymes *Nco*I and *Bam*HI and ligated to the vector pTrc99A, digested with the same enzymes. Recombinants were selected after transformation into the *E. coli* strain DH5α on the basis of super coiled plasmid mobility [39]. The presence of insert was confirmed by restriction digestion whose sites were incorporated in the mutagenic primers. The clones were sequenced to confirm the mutation (Microsynth, Switzerland).

Protein expression and purification

Expression of the TIM gene was performed using the pTrc99A system. *E. coli* AA200 (a null mutant of inherent TIM gene) cells carrying the pTrc99A- recombinant vector were grown at 37 °C in Terrific broth containing 100 μg/ml ampicillin. Cells were induced using 300 μM IPTG (isopropyl-β-D-thiogalactopyranoside) at 0.6-0.8 OD_{600nm} and were harvested by centrifugation (15 min, 6K rpm, 4°C). Cells were resuspended in lysis buffer, containing 20 mM Tris-HCl (pH 8.0), 1 mM EDTA, 0.01 mM PMSF, 2 mM DTT and 10% glycerol and disrupted using sonication. After centrifugation (45 min, 12K rpm, 4°C), the supernatant was fractionated by ammonium sulfate. The protein fraction containing TIM was precipitated between 60-80% ammonium sulphate saturation. This precipitate was collected by centrifugation (30 min, 12K rpm, 4°C) and resuspended in buffer-A [20 mM Tris-HCl (pH 8.0), 2 mM DTT, and 10% glycerol]. Monitoring of each step was performed by SDSPAGE analysis (12% polyacrylamide). Nucleic acid was removed using PEI (polyethyleneimine) precipitation and the succeeding purification steps were conducted at 4°C. The protein was dialyzed extensively against buffer-A at

4°C overnight and purified using an anion exchange (Q- sepharose, HR 60) column and eluted with a linear gradient of 0 - 1M NaCl. The fractions containing the protein were pooled and precipitated by addition of ammonium sulfate upto a concentration of 75%. The precipitated protein was dissolved in buffer-A and subjected to gel filtration chromatography (Sephacryl-200), equilibrated with the same buffer on an AKTA BASIC FPLC system. Protein purity was checked by 12% SDS-PAGE and all preparations used at were least 95% pure. Protein purity was also verified by ESI mass spectrometry. Protein concentration was determined by the Bradford's method [40] using BSA as a standard.

Enzyme activity

The enzyme activity of TIM was determined by the conversion of GAP (glyceraldehyde-3-phosphate) to DHAP (dihydroxyacetone phosphate) in the presence of TIM and α-glycerophosphate dehydrogenase [41, 42]. Enzymes were freshly prepared in 100 mM triethanolamine-HCl (TEA pH 7.6). The reaction mixture contained (final volume 1ml) 100 mM TEA, 5 mM EDTA, 0.5 mM NADH and α-glycerophosphate dehydrogenase (20 μg ml^{-1}) and 0.1-3 mM glyceraldehyde 3- phosphate. Enzyme activity was determined by monitoring the decrease in absorbance at 340 nm. The dependence of the initial rate on the substrate concentration was analyzed according to the Michaelis-Menten equation. The values of the kinetic parameters (K_m, k_{cat}) were calculated from Lineweaver-Burke plots.

Size exclusion chromatography

Analytical gel filtration was performed on a Superdex-200 column (300 × 10mm) attached to an AKTA BASIC FPLC system at a flow rate of 0.5 ml min^{-1} and protein elution was monitored at a wavelength of 280 nm. The column was calibrated with β-amylase (200 kDa), alcohol dehydrogenase (150 kDa), bovine serum albumin (66 kDa), carbonic anhydrase (29 kDa) and cytochrome C (12.4 kDa).

Mass spectrometry

Electrospray ionization mass spectra were recorded on an Esquire 3000+ series mass spectrometer (Bruker Daltonics) coupled to an online 1100 series HPLC. Nebulisation was assisted by N_2 gas (99.8%) at a flow rate of 10 L min^{-1}. The spray chamber was held at 250-300°C. The spectrometer was tuned to five calibration standards provided by the manufacturer. Data processing was done using the deconvolution module of the data analysis software to detect the multiple charge states and obtain derived masses.

Fluorescence spectroscopy

Fluorescence emission spectra were recorded on a HITACHI-250 spectroflorimeter. The protein samples were excited at 280 nm or 295 nm separately, and the emission spectra recorded from 300 nm to 400 nm. Excitation and emission band passes were kept as 5 nm. Denaturation studies were done incubating 5 μM protein with different concentration of urea and GdmCl for 45-60 min and individual spectra were acquired from 300-450 nm after exciting the molecule at 295 nm.

Circular dichroism (CD) spectroscopy

Far UV-CD measurements were carried out on a JASCO-715 spectro-polarimeter equipped with a thermostatted cell holder. The temperature of the sample solution in the cuvette was controlled with a peltier device. For thermal melting studies, ellipticity changes at 222 nm were monitored to follow the unfolding transition. A cuvette of path length of 1 mm was used and the spectra were averaged over four scans at a scanning speed of 10 nm min^{-1}. The change of ellipticity was measured as a function of temperature for thermal melting. Denaturation studies were done by incubating 5 μM of protein with different concentrations of urea and GdmCl for 45-60 min and individual spectra (250-200 nm) were averaged out over three scans.

Structure visualization

All structural superpositions were carried out by secondary structure matching [43] using COOT [44]. Hydrogen bonds and van der Waals contacts were identified using the CONTACT program of CCP4 suite based on distance criteria of 3.5 and 4.0 Å, respectively. The figures were generated using PyMol [45].

Acknowledgements

The mass spectral facility was supported under the Proteomics program of the DBT. MB was a Senior Research Fellow of the Council for Scientific and Industrial Research, Government of India. This research was supported by program grants from Department of Biotechnology (DBT) and Department of Science and Technology (DST), Senior Research Fellowships of the Council for Scientific and Industrial Research (CSIR), Government of India.

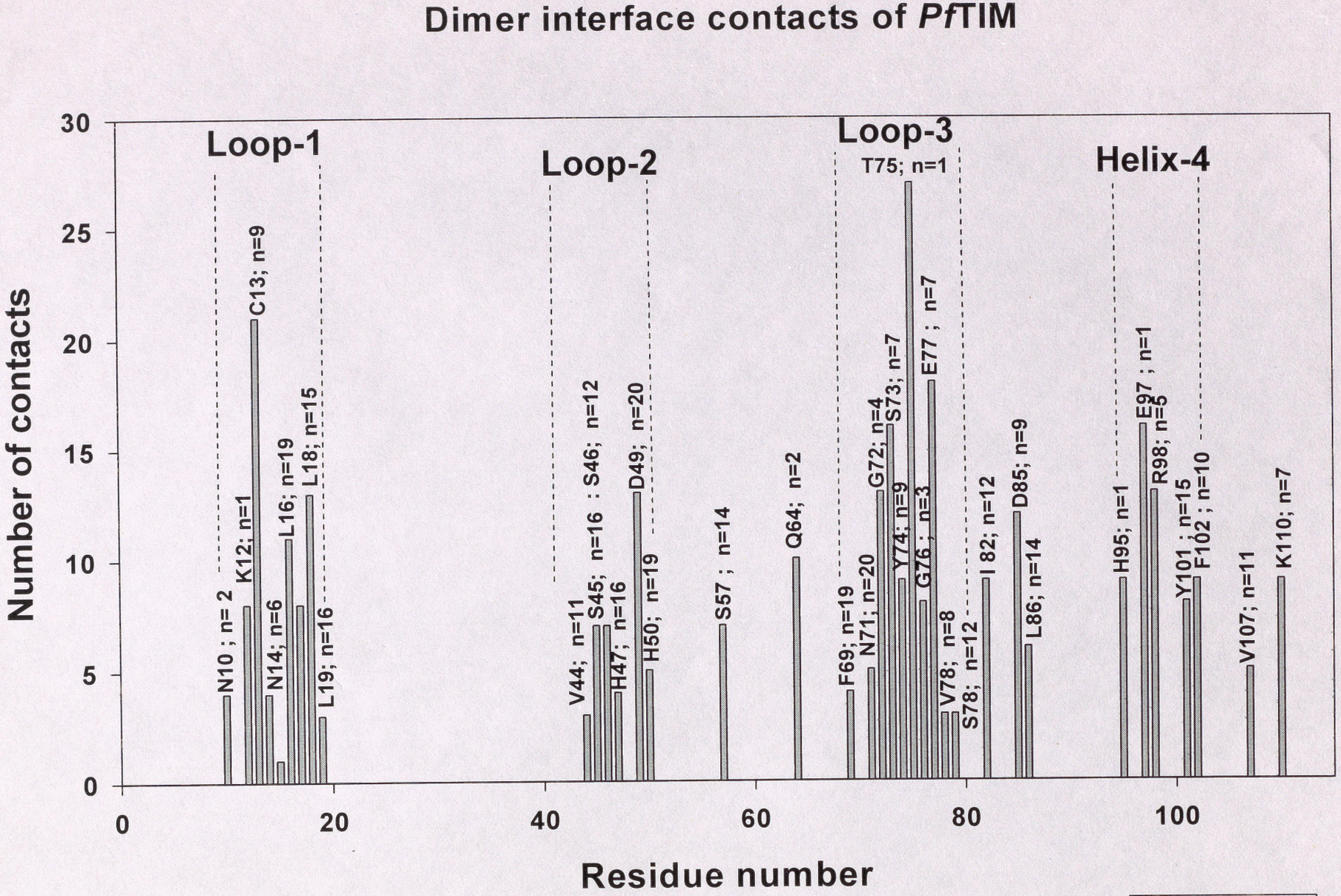
Dimer interface contacts of PfTIM
Number of contacts
Residue number
Loop-1
Loop-2
Loop-3
Helix-4
N10 ; n= 2
K12; n=1
C13; n=9
N14; n=6
L16; n=19
L18; n=15
L19; n=16
V44; n=11
S45; n=16
: S46; n=12
H47; n=16
D49; n=20
H50; n=19
S57 ; n=14
Q64; n=2
F69; n=19
N71; n=20
G72; n=4
S73; n=7
T75; n=1
Y74; n=9
G76 ; n=3
E77 ; n=7
V78; n=8
S78; n=12
I 82; n=12
D85; n=9
L86; n=14
H95; n=1
E97 ; n=1
R98; n=5
Y101 ; n=15
F102 ; n=10
V107; n=11
K110; n=7

Figure 1

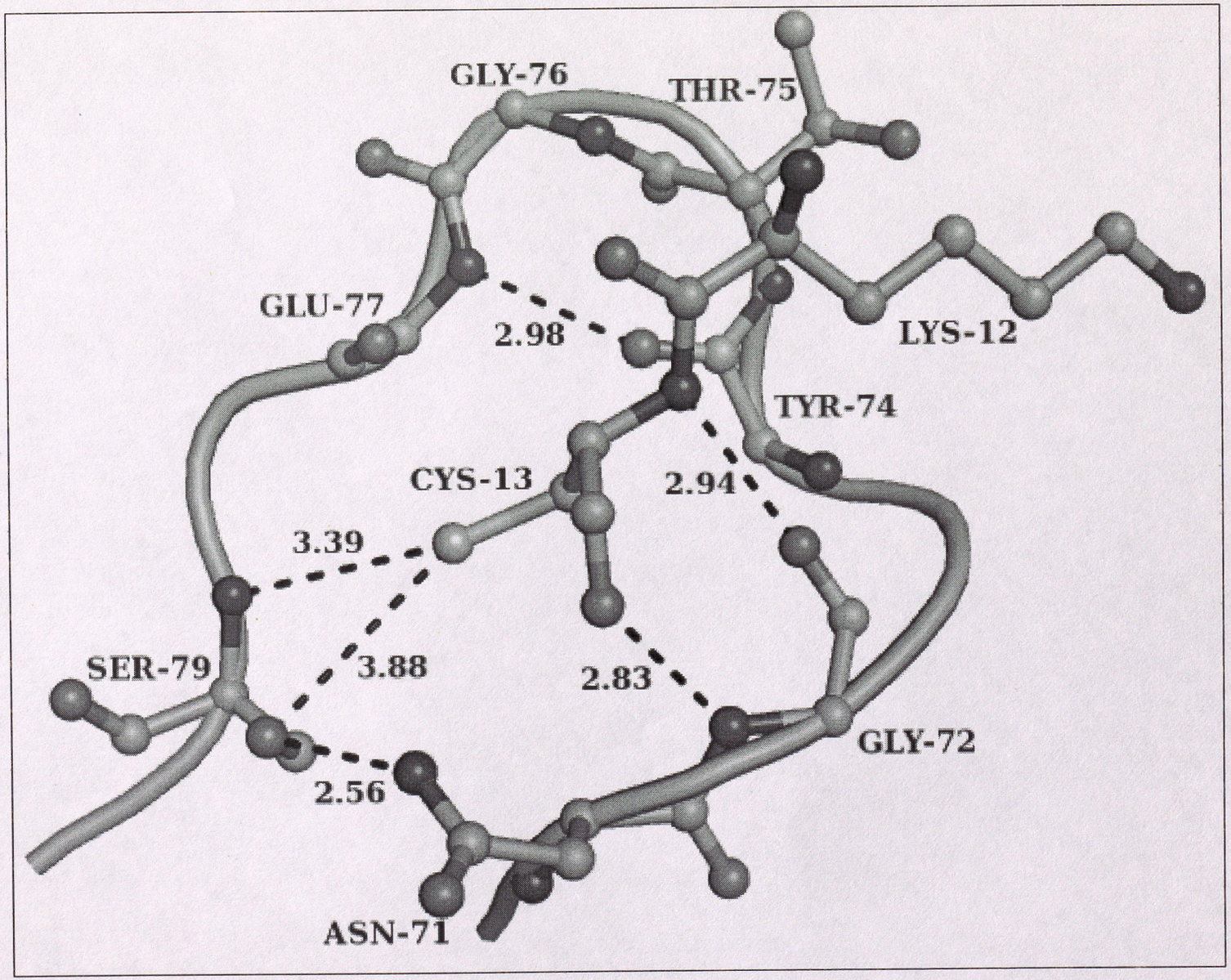
GLY-76
THR-75
GLU-77
2.98
LYS-12
TYR-74
CYS-13
2.94
3.39
SER-79
3.88
2.83
GLY-72
2.56
ASN-71

Figure 2

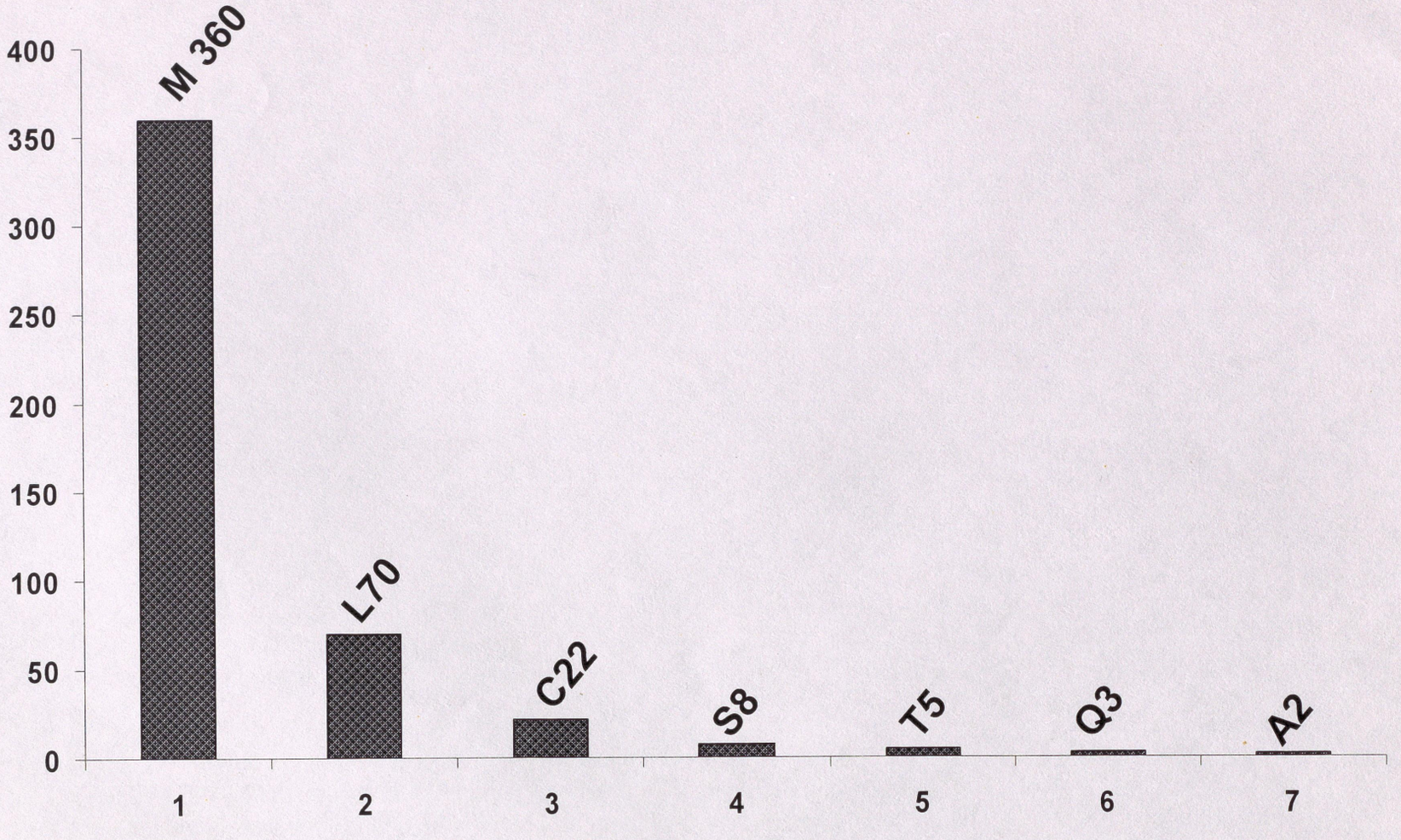

Figure 2 (inset)

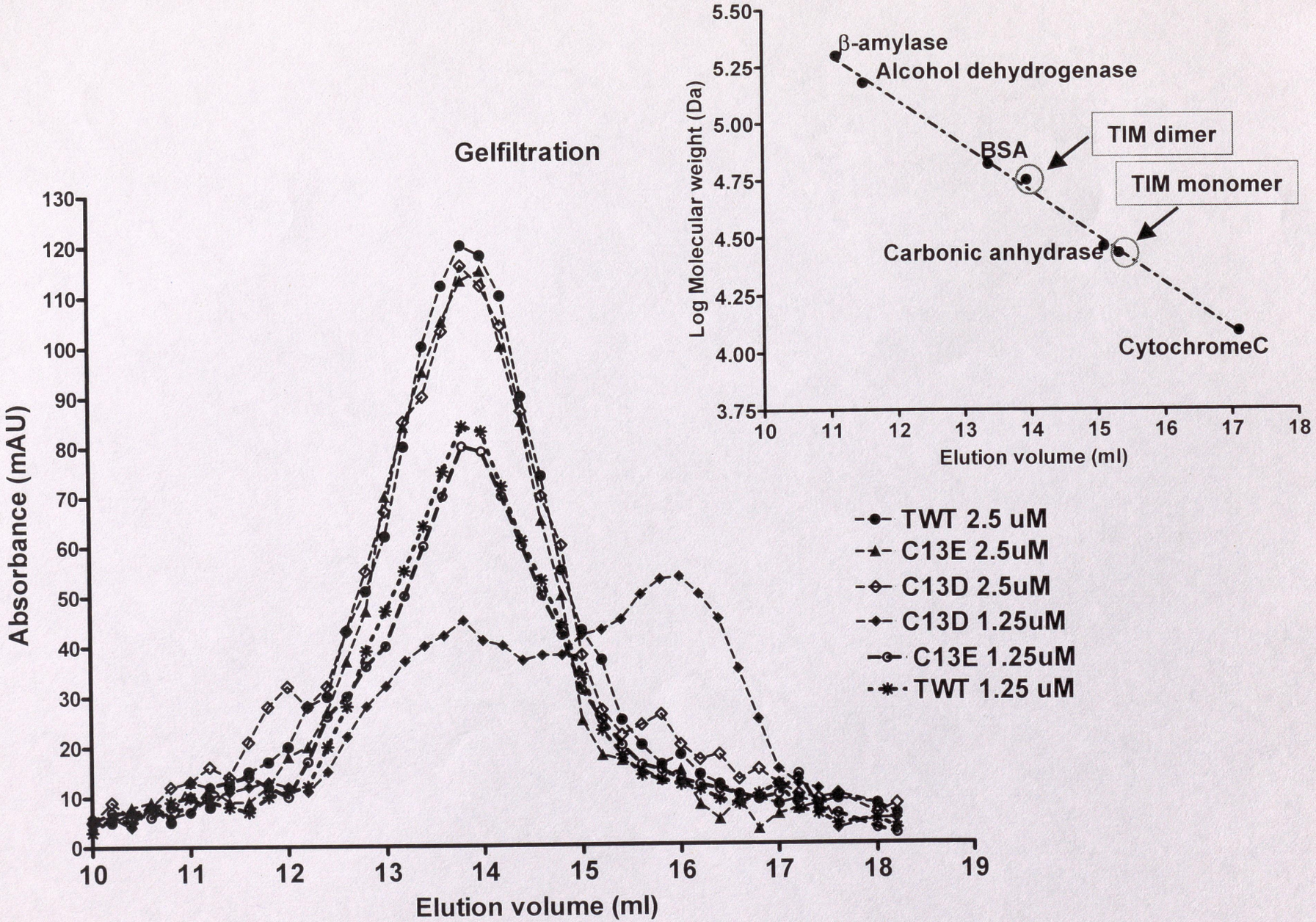
Gelfiltration
Absorbance (mAU)
Elution volume (ml)
TWT 2.5 uM
C13E 2.5uM
C13D 2.5uM
C13D 1.25uM
C13E 1.25uM
TWT 1.25 uM
Log Molecular weight (Da)
β-amylase
Alcohol dehydrogenase
BSA
TIM dimer
TIM monomer
Carbonic anhydrase
CytochromeC
Elution volume (ml)

Figure 3

Figure 4

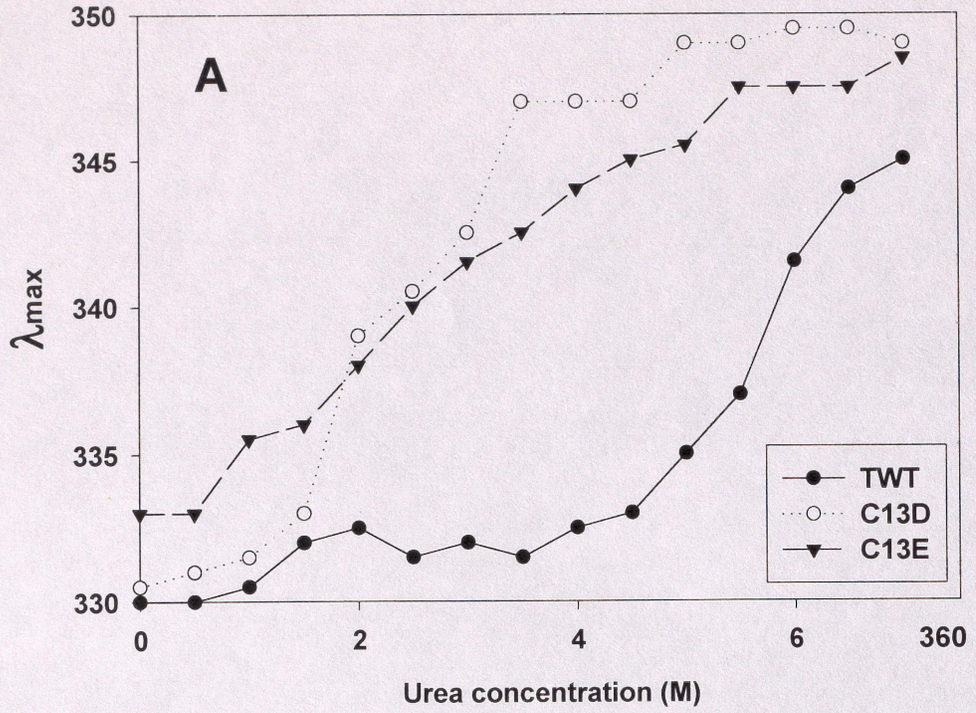

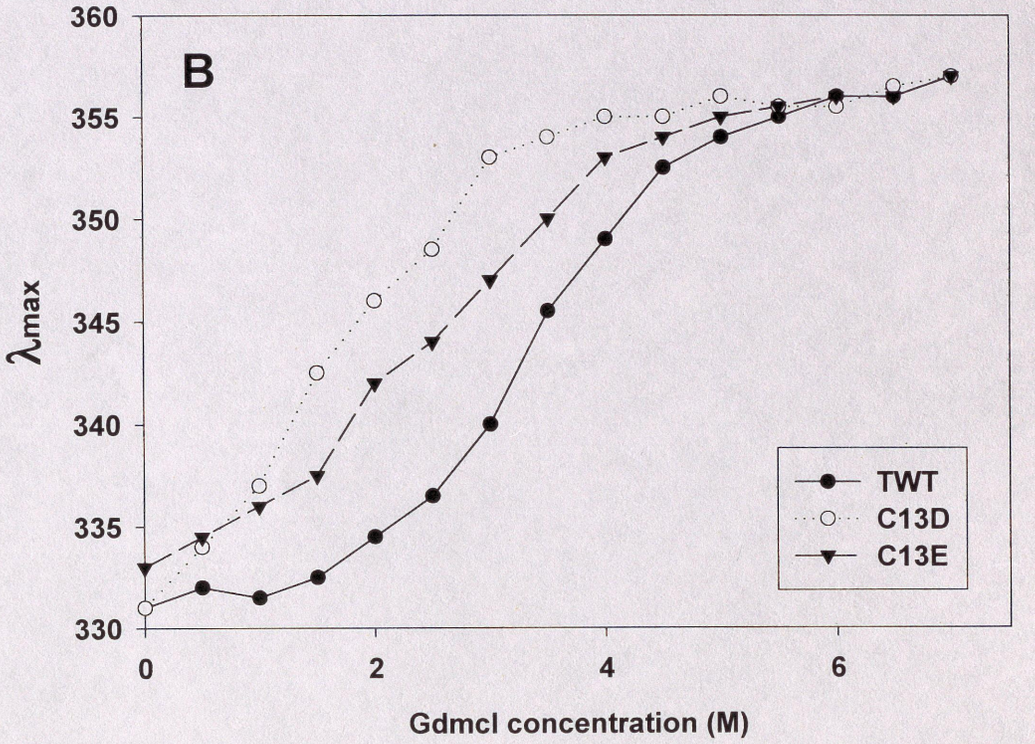

Fluorescence

Figure 4

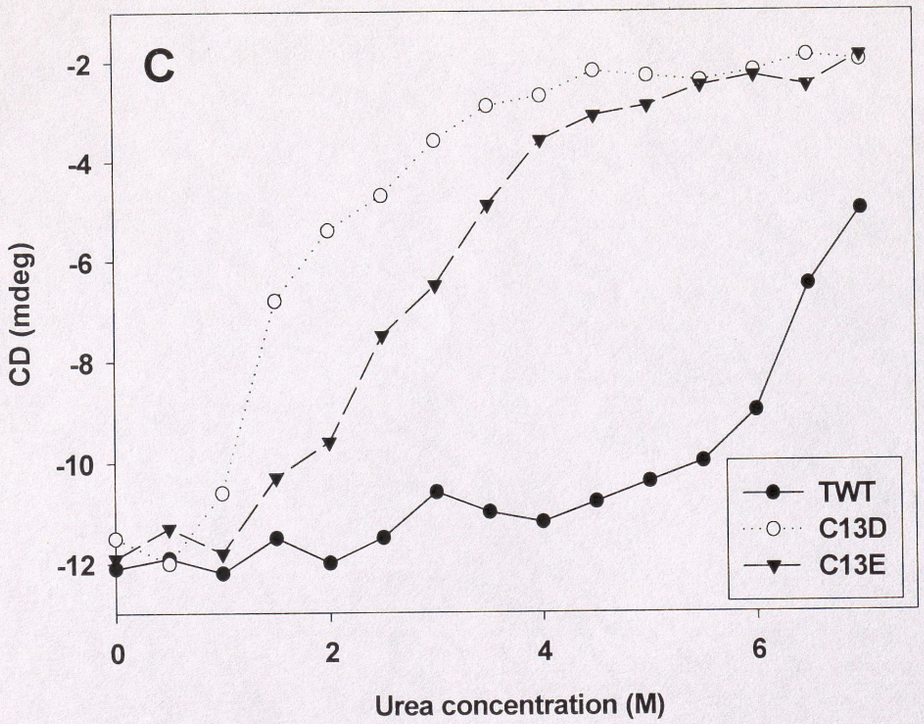

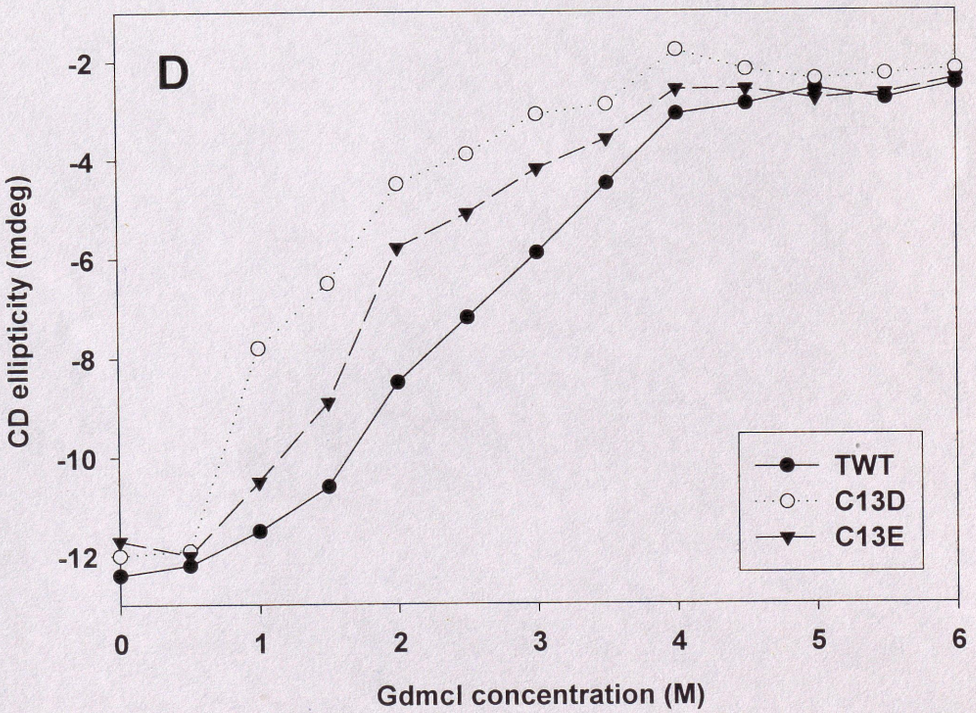

Circular dichroism

Thermal denaturation

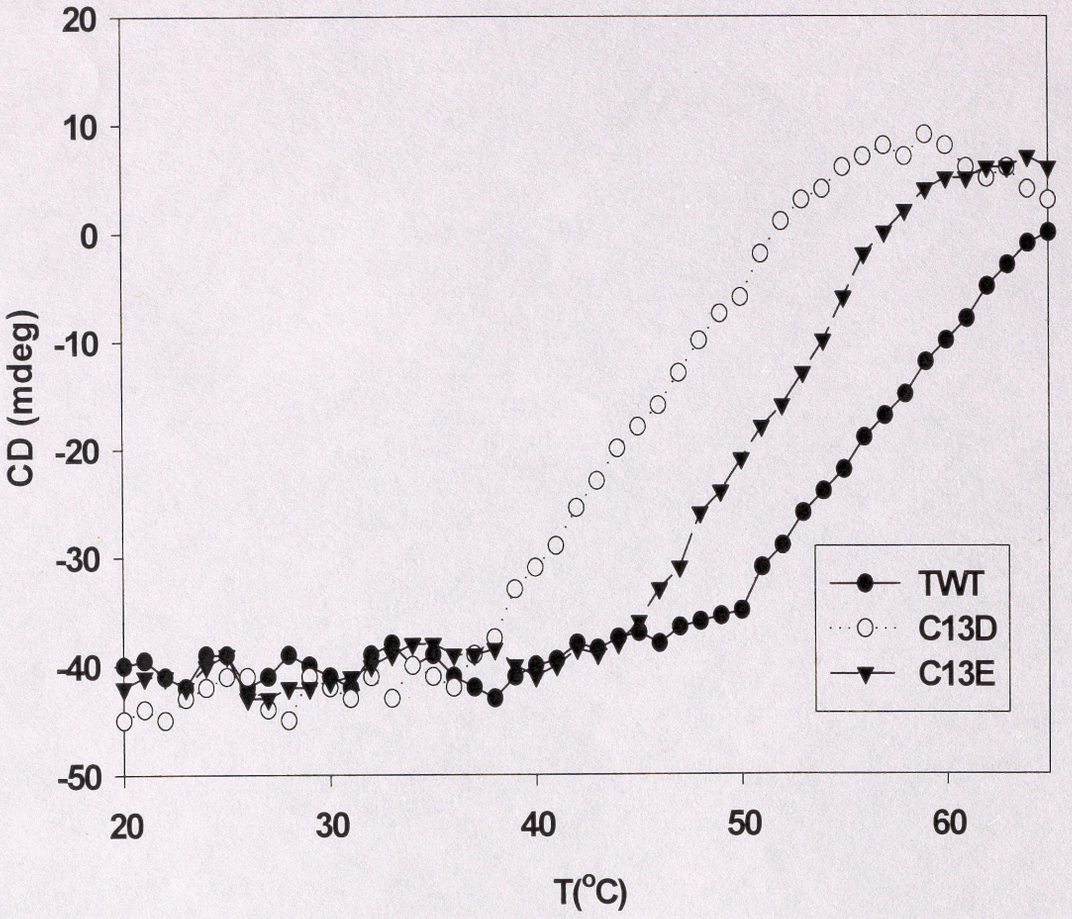

Figure 5

T75 environment

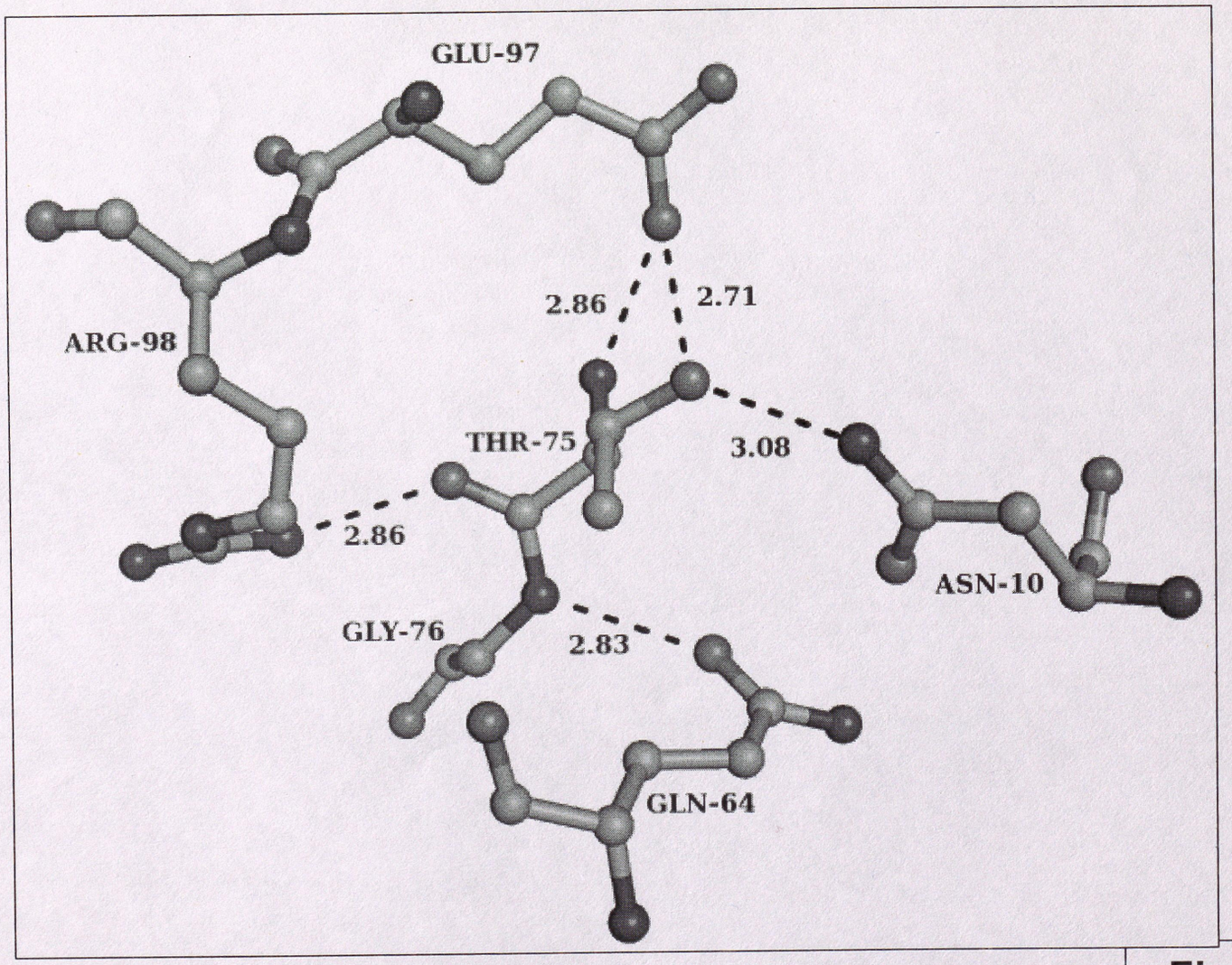

Figure 6

13-71-79-82

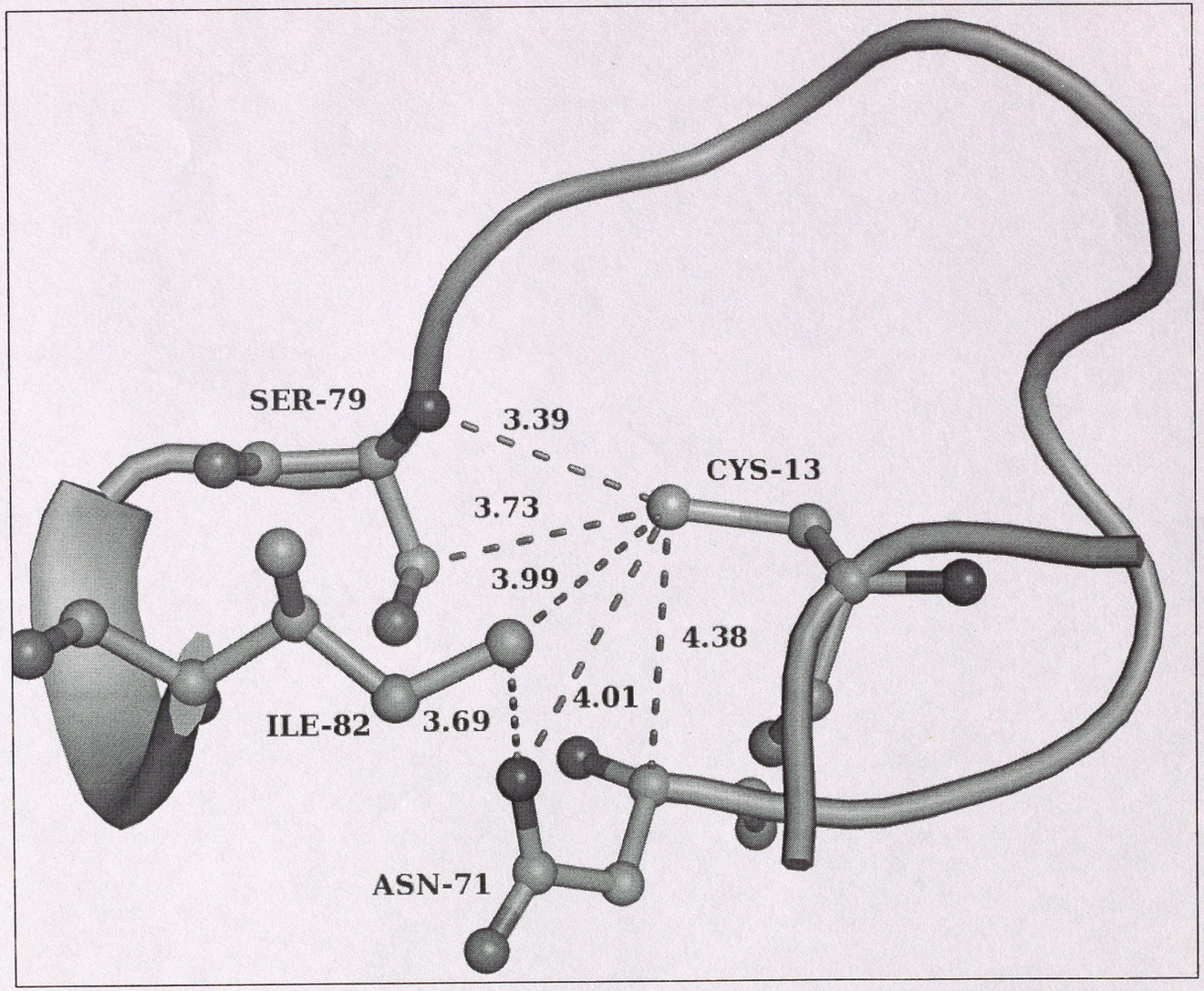

Figure 7

Figure 8

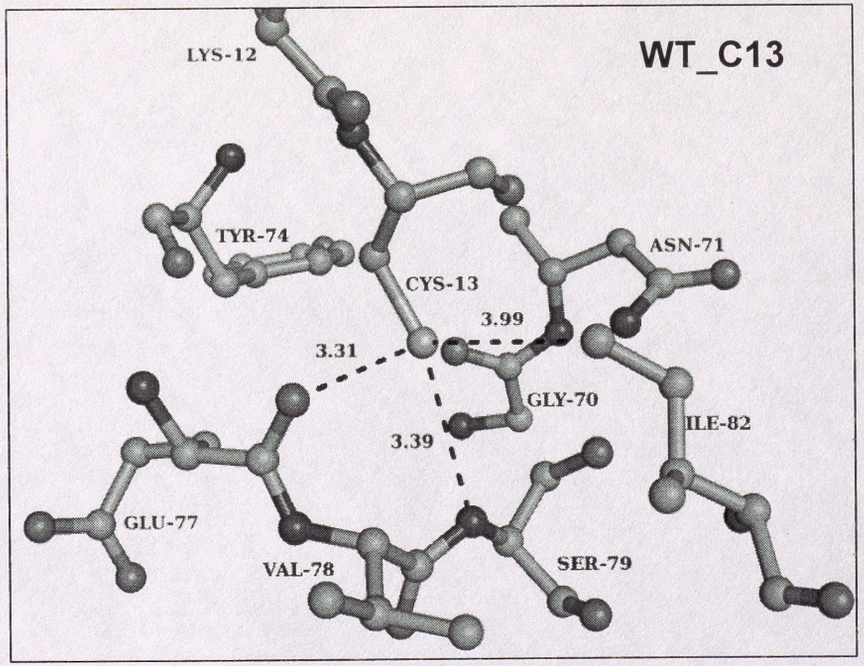
WT_C13
LYS-12
TYR-74
CYS-13
ASN-71
3.99
3.31
GLY-70
ILE-82
3.39
GLU-77
VAL-78
SER-79

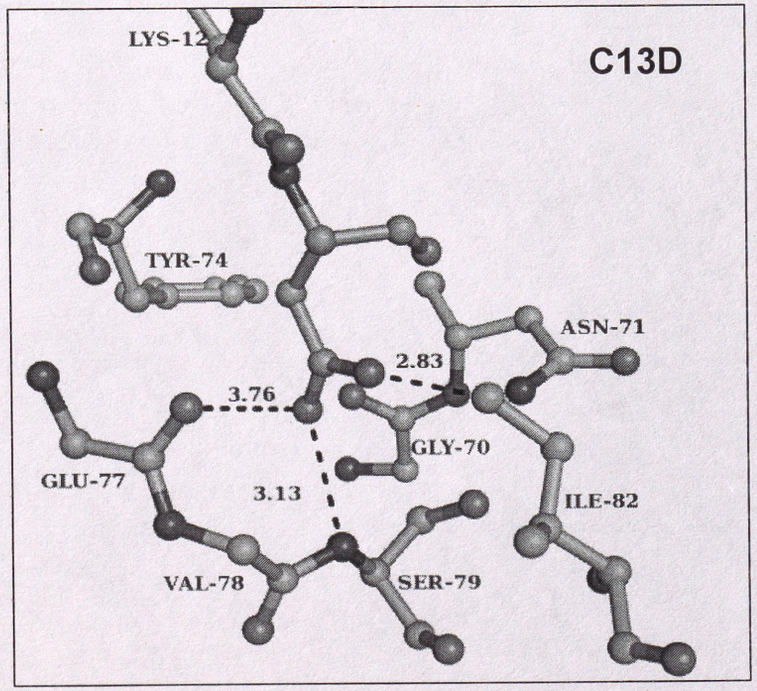
C13D
LYS-12
TYR-74
ASN-71
2.83
3.76
GLY-70
GLU-77
3.13
ILE-82
VAL-78
SER-79

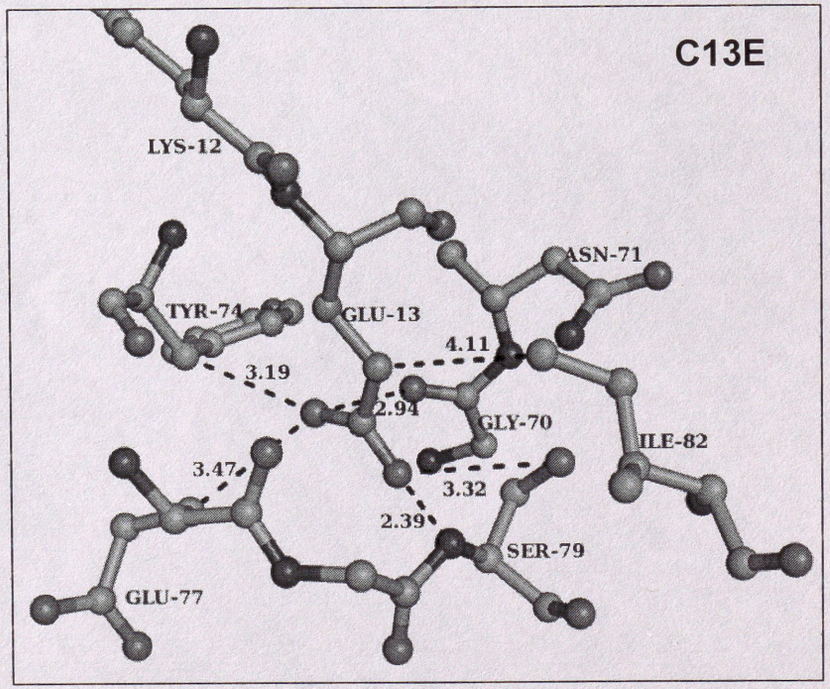
C13E
LYS-12
ASN-71
TYR-74
GLU-13
4.11
3.19
2.94
GLY-70
ILE-82
3.47
3.32
2.39
SER-79
GLU-77

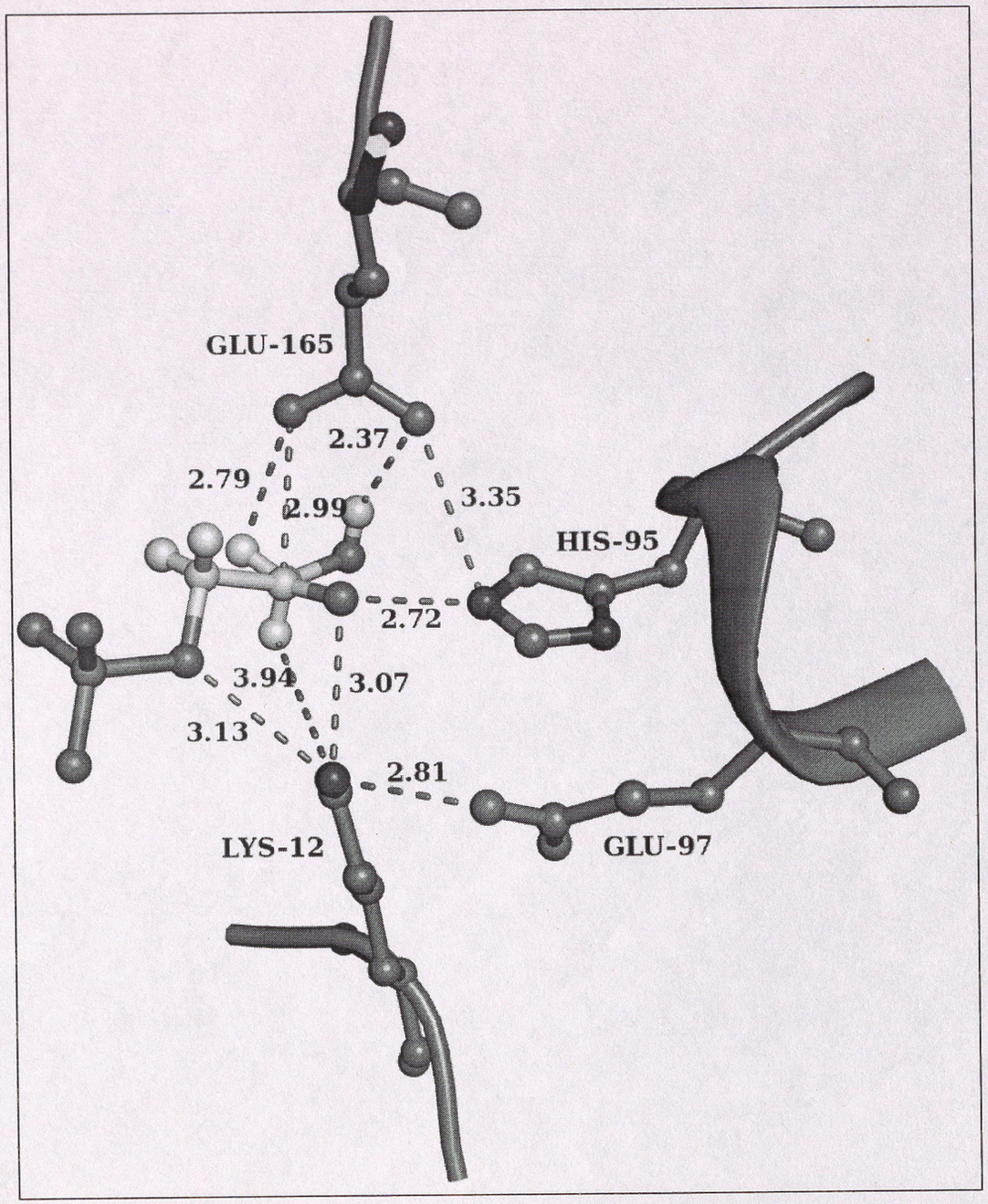
GLU-165
2.37
2.79
2.99
3.35
HIS-95
2.72
3.94
3.07
3.13
2.81
LYS-12
GLU-97

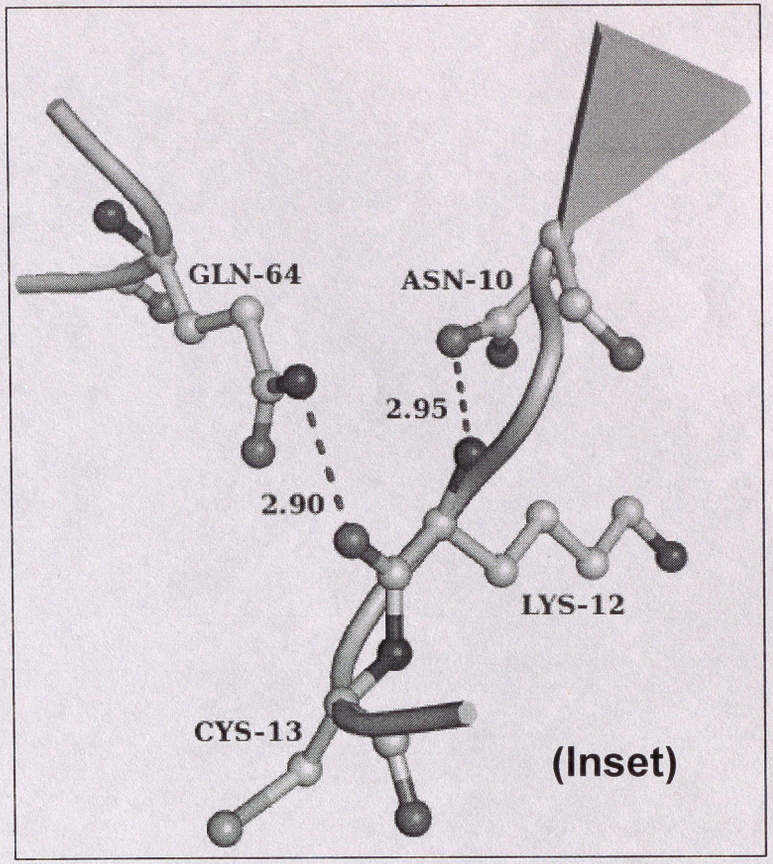
GLN-64
ASN-10
2.95
2.90
LYS-12
CYS-13
(Inset)

Figure 9

k_{cat} of TIM from different organisms

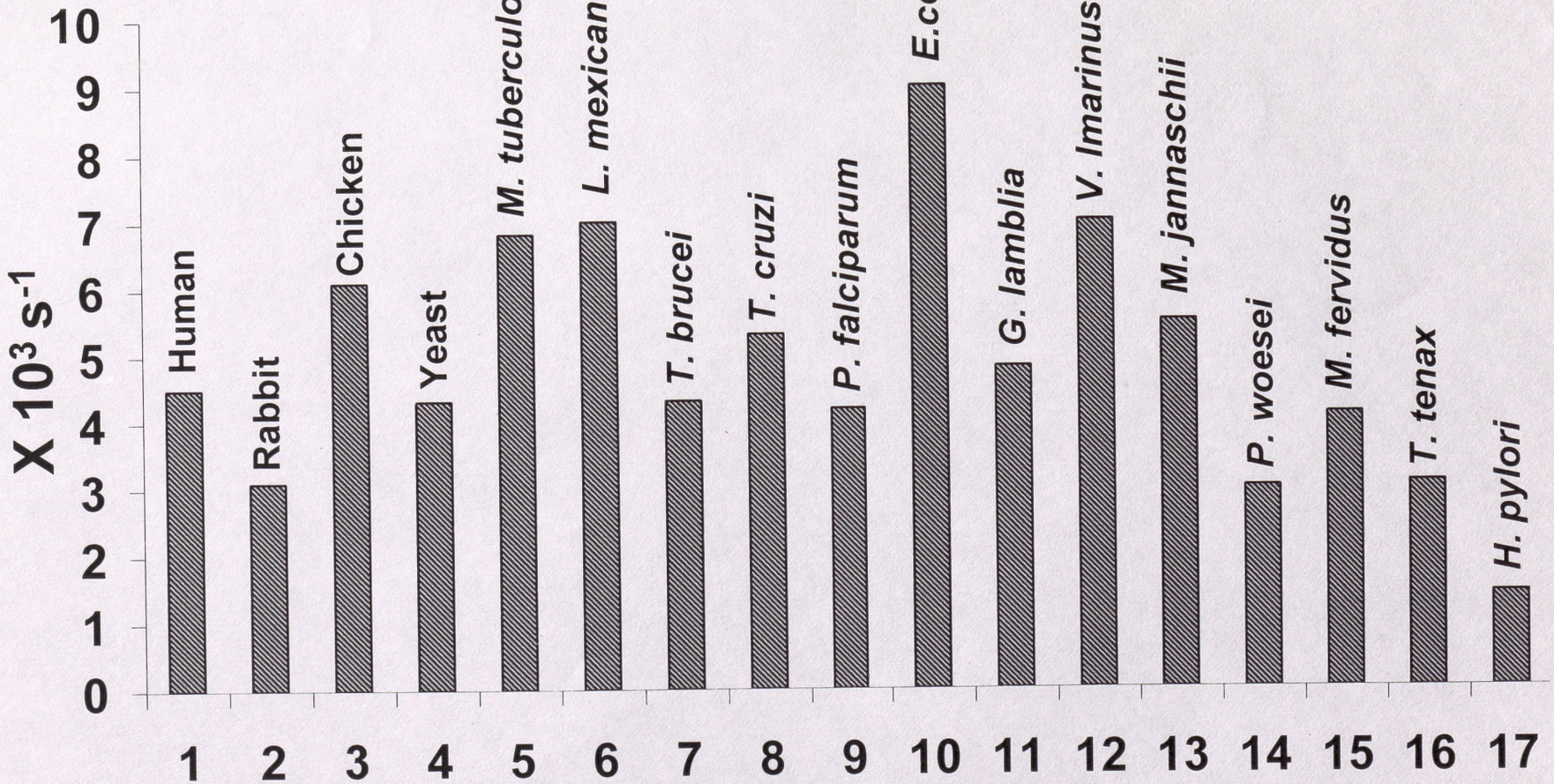

$k_{cat} = 4.90 \pm 1.86\ s^{-1}$

Figure 10

K_m of TIM from different organisms

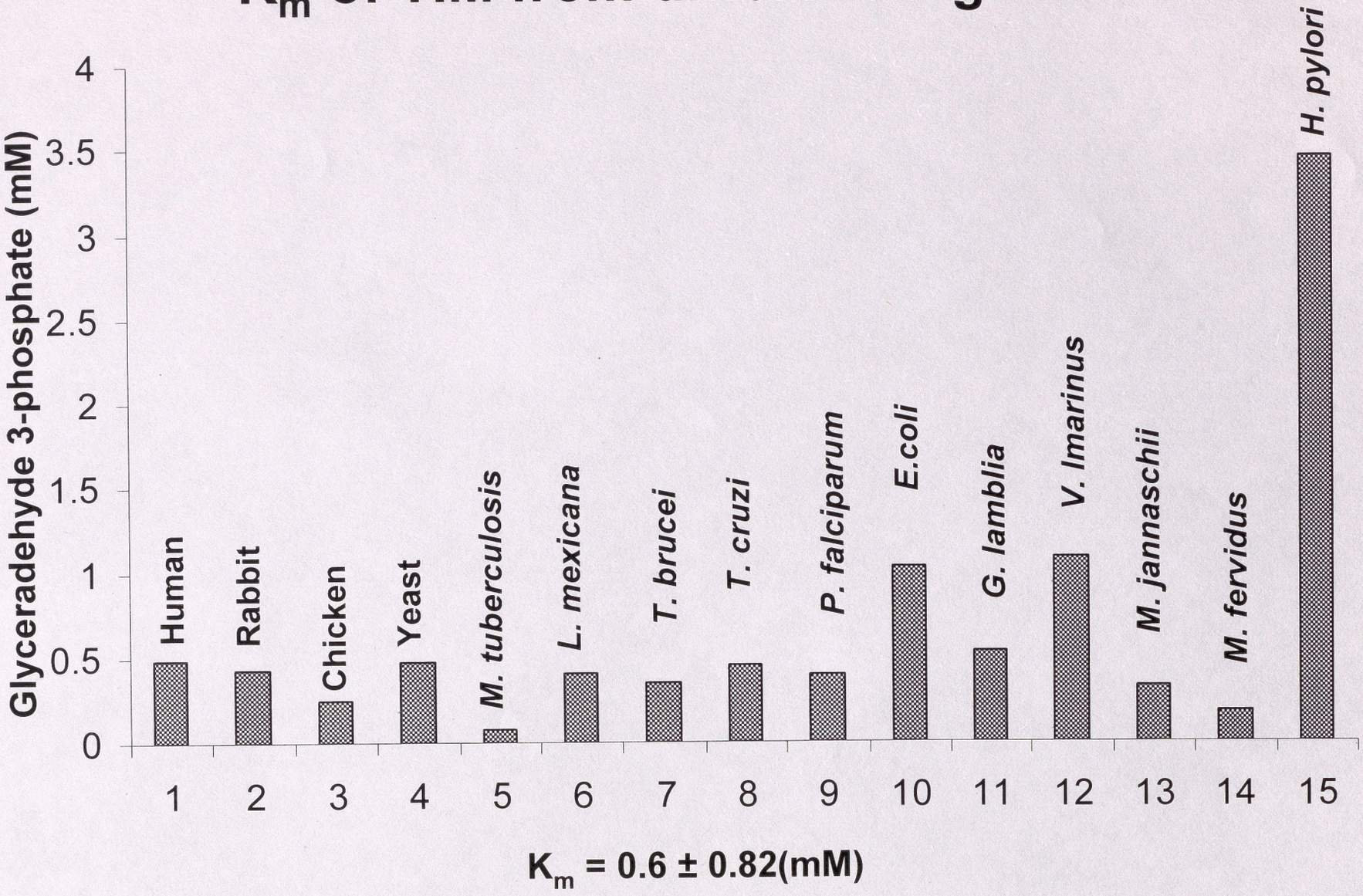

$K_m = 0.6 \pm 0.82(mM)$

Figure 10B

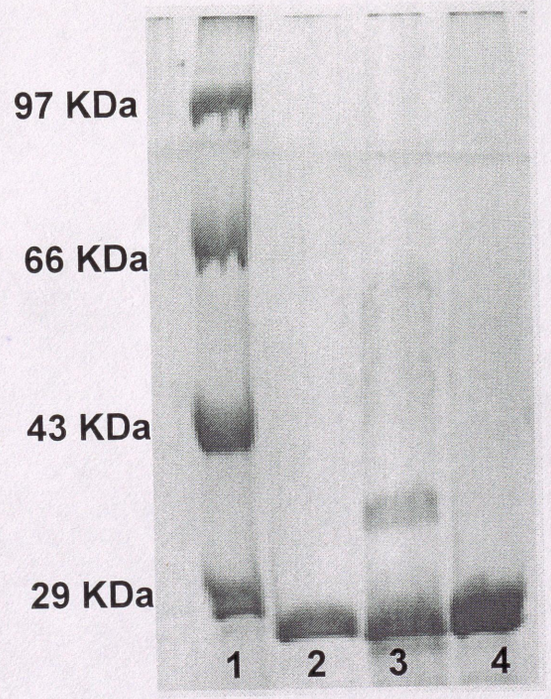

Figure S1

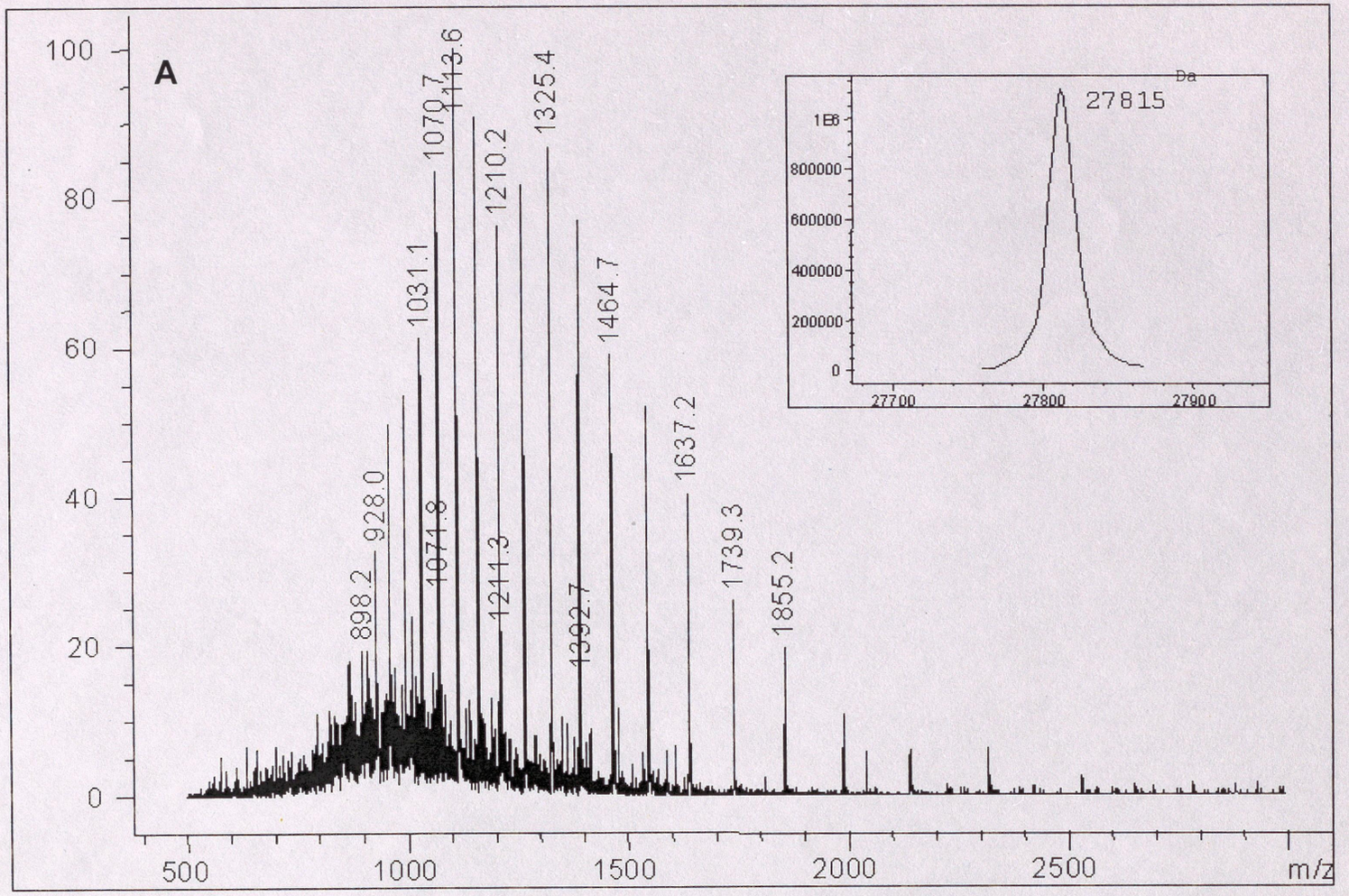
A
100
80
60
40
20
0
898.2
928.0
1031.1
1070.7
1113.6
1074.8
1210.2
1211.3
1325.4
1392.7
1464.7
1637.2
1739.3
1855.2
500
1000
1500
2000
2500
m/z
1E6
800000
600000
400000
200000
0
27700
27800
27900
Da
27815

Figure S2A

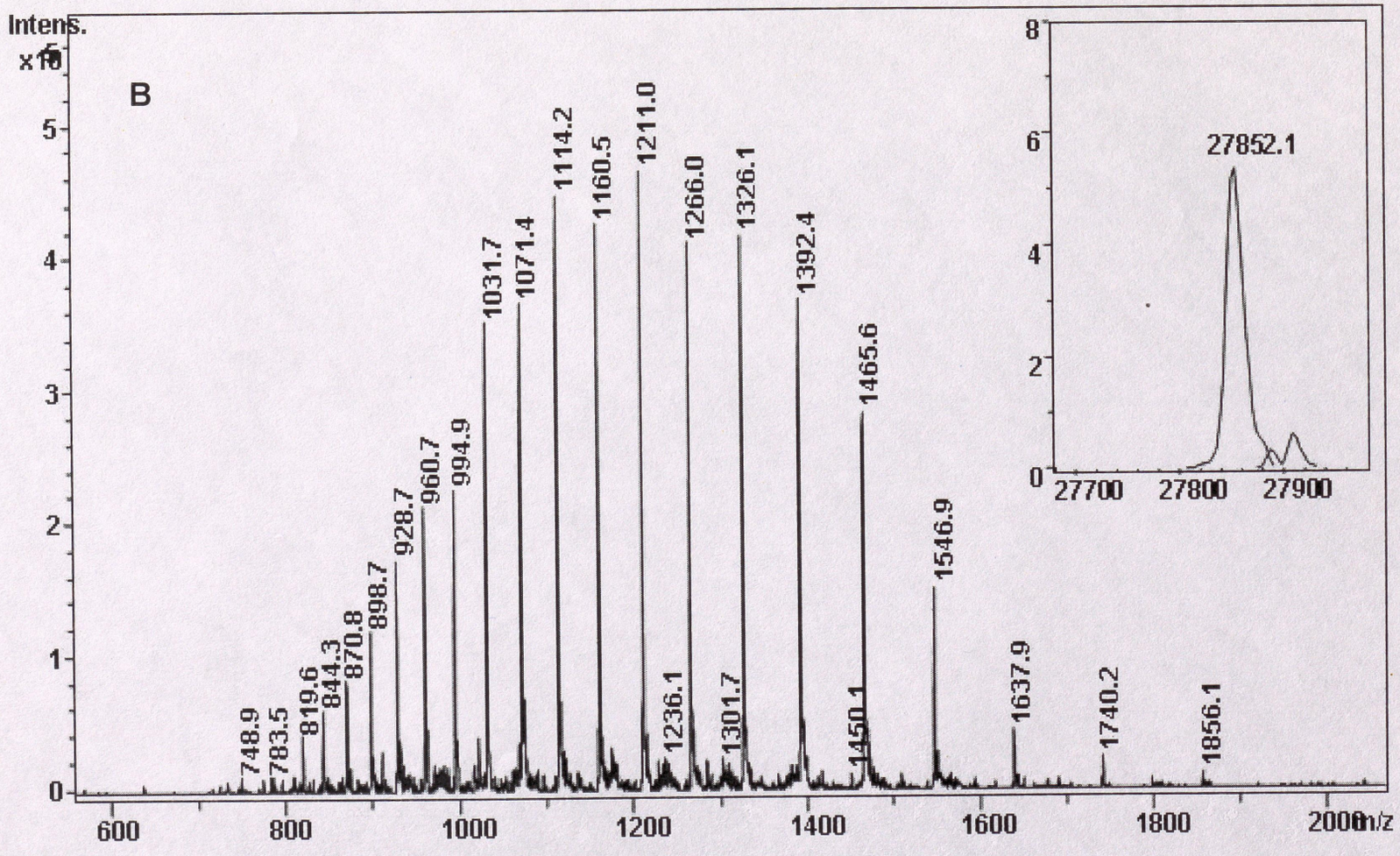
Intens.
x10
B
748.9
783.5
819.6
844.3
870.8
898.7
928.7
960.7
994.9
1031.7
1071.4
1114.2
1160.5
1211.0
1236.1
1266.0
1301.7
1326.1
1392.4
1450.1
1465.6
1546.9
1637.9
1740.2
1856.1
27852.1
m/z

Figure S2B

C13D enzyme activity

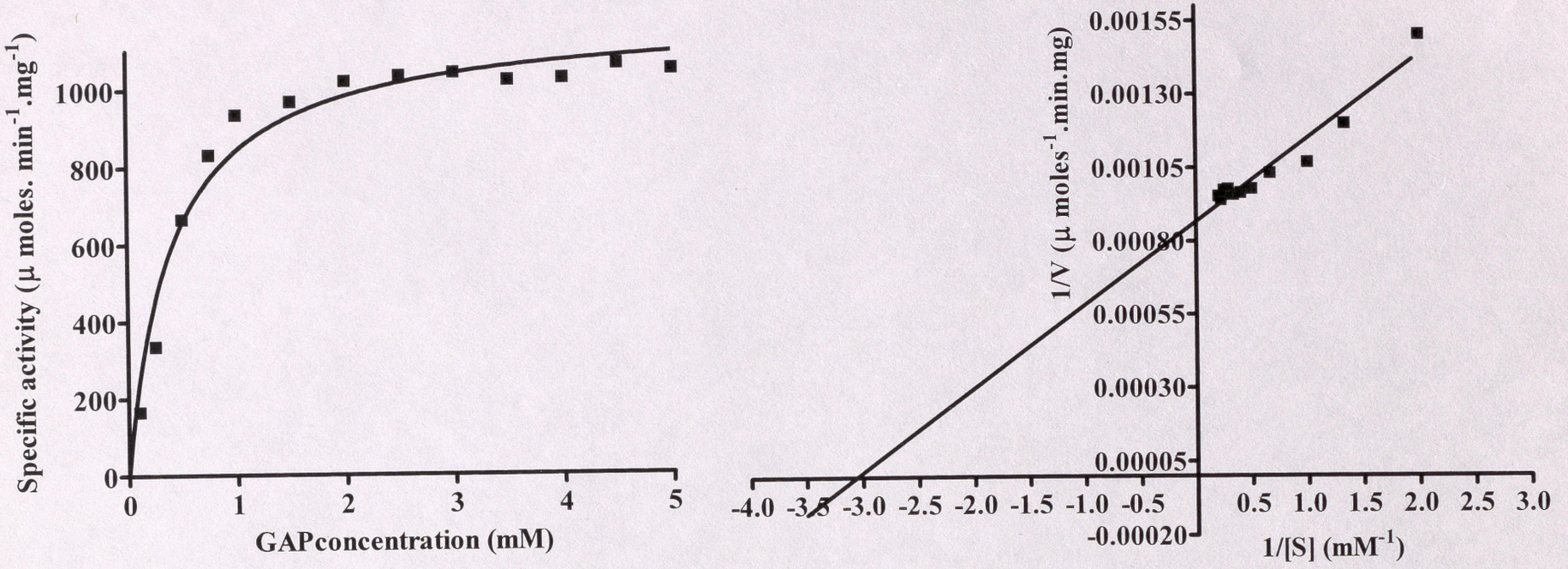

Figure S3A

C13E enzyme activity

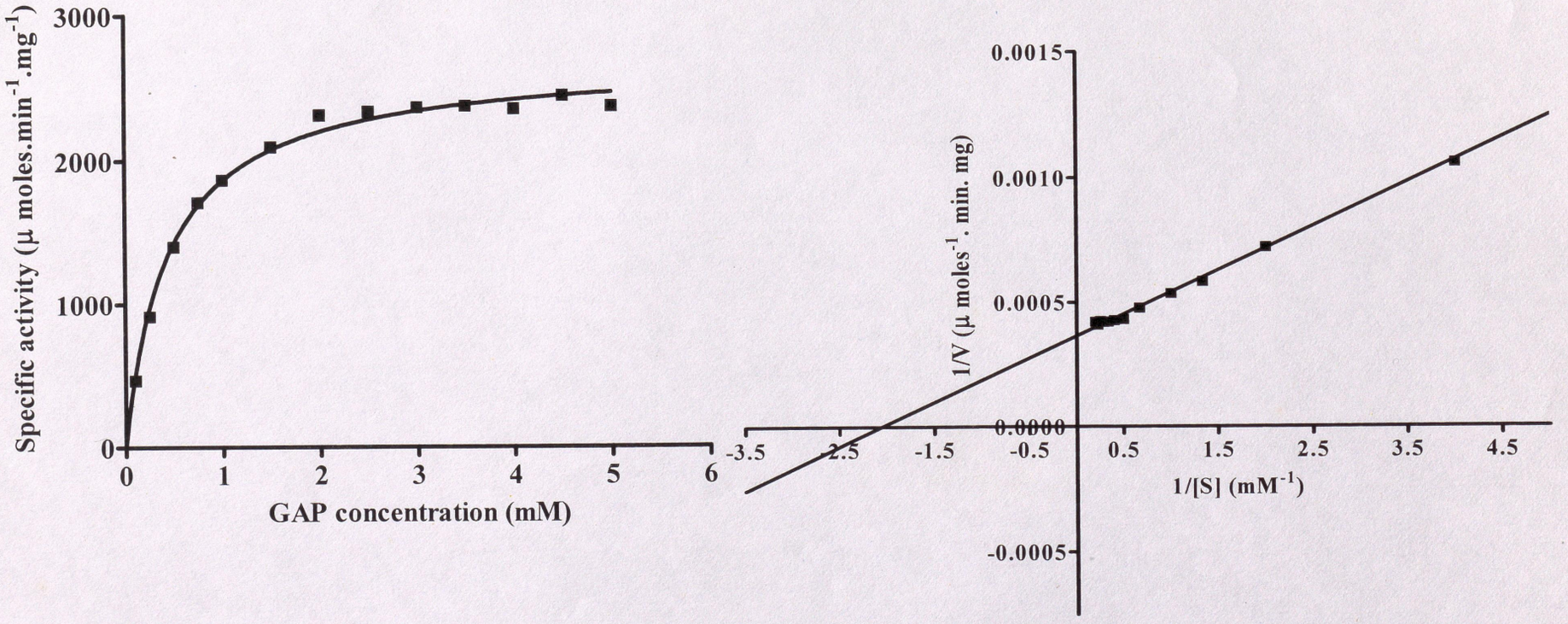

Figure S3B